Contact Lens and Anterior Eye 42 (2019) 325–333

Contents lists available at ScienceDirect

Contact Lens and Anterior Eye

journal homepage: www.elsevier.com/locate/clae

Short communication

Antimicrobial and physicomechanical natures of silver nanoparticles incorporated into silicone-hydrogel films

Reda Mourad[a,*], Fahima Helaly[a], Osama Darwesh[b], Sanaa El- Sawy[a]

[a] Department of Polymers and Pigments, National Research Centre, Dokki, Cairo, Egypt
[b] Department of Agricultural Microbiology, National Research Centre, Dokki, Cairo, Egypt

ARTICLE INFO

Keywords:
Silicone-hydrogel
Contact lenses
Antimicrobial
AgNPs
Cytoxicity

ABSTRACT

Purpose: The effects of silver nanoparticles (AgNPs) incorporated in silicone-hydrogel films on their physico-chemical properties and microbial activity were investigated.

Methods: Silicone-hydrogel composite films (SiHCFs) were prepared by *in-situ* chemical reduction of silver ions added in different concentrations (0, 10, 20, 30, 40, 60, and 80 ppm) followed by ultraviolet (UV) casting. The reduction of silver ions into AgNPs was confirmed by transmission electron microscopy (TEM) and absorption spectroscopy over ultraviolet and visible (UV–vis) wavelengths. Incorporation of AgNPs into SiHCFs was confirmed by UV–vis absorption spectroscopy, scanning electron microscopy (SEM), and energy-dispersive X-ray (EDX) spectroscopic mapping. The physico- mechanical properties of the SiHCFs were evaluated. Antimicrobial activity and biofilm formation of *Escherichia coli, Pseudomonas aeruginosa, and Staphylococcus aureus* were assessed.

Results: TEM, UV–vis absorption, SEM, and EDX mapping showed that silver ions were reduced in the mixture of co-polymerizing monomers and incorporation of AgNPs into SiHCFs was achieved. Mechanical properties of the SiHCFs were enhanced with increasing AgNPs concentration without affecting their chemical and thermal properties. SiHCFs exhibited transmittance greater than 90% at a wavelength 600 nm. Bacterial growths in the solutions bathing the SiHCFs with increasing silver concentration were 95, 78, 4, 2, 0, 0, 0% respectively, for *Escherichia coli*; 95, 82, 4, 0.6, 0, 0, 0% for *Pseudomonas aeruginosa*; and 93, 79, 4, 0.5, 0, 0, 0% for *Staphylococcus aureus*.

Conclusions: Incorporation of AgNPs into SiHCFs demonstrated sufficient release of AgNPs to inhibit bacterial growth and reduce biofilm formation, with collateral enhancement of some mechanical properties of SiHCFs.

1. Introduction

Silicone-hydrogel contact lens wear is associated with microbialkeratitis accompanied by acute red eye and induced peripheral ulcers [1]. Microbial keratitis can promote from infections caused by bacteria (*Staphylococcus aureus, Pseudomonas Aeruginosa*, etc.) and fungi (*Candida, Aspergillums, Fusarium*, etc.) [2–5]. A contact lens can possess antimicrobial properties by incorporation of antimicrobial agents infused into the bulk o r on the surface of the lens to decrease the risk of microbial keratitis [6–8]. Many attempts have been developed to introduce new antimicrobials overcoming antibiotic resistance. One of the novel methods to do so is dispersing antimicrobial nanomaterials into hydrogels homogeneously. Such nanoparticle containing hydrogels are called nanocomposites. Several works have focused on gold and silver as remarkable choice for antimicrobial agents development [9–11]. Silver nanoparticles (AgNPs) are considered antimicrobial agents and have been incorporated in polymers to achieve antibacterial effects [12,13]. AgNPs have a broad-spectrum antimicrobial effect. The action of AgNPs is uncertain but, there is some proposed mechanisms such as disruption of the cell membrane, inactivation and modification of enzyme structure, interference with cell respiration or with DNA and RNA preventing cells multiplication [14]. The antibacterial action of AgNPs impregnated soft contact lenses has been studied in *in vitro*. It was found that the increase of AgNPs loading enhanced the antibacterial activity of the hydrogel [6,15,16]. On the other hand, it is important to enhance hydrogels with proper mechanical toughness, elasticity and transparency. Kazutoshi et al. [17], demonstrated that the mechanical properties greatly increased by adding inorganic nano-clays and showed that the clay sheet acts as a cross-linking agent for the polymer. Zhao et al. [18], also found that the young's modulus of poly

* Corresponding author.
E-mail addresses: rmmay80@yahoo.com, redamourad14@gmail.com (R. Mourad).

https://doi.org/10.1016/j.clae.2019.02.007
Received 15 November 2018; Received in revised form 21 January 2019; Accepted 18 February 2019
1367-0484/ Published by Elsevier Ltd on behalf of British Contact Lens Association.

(vinyl alcohol) hydrogel increased to nearly 10 times with graphene loading of 1.8 vol%. Huang et al. [19], designed a hybrid hydrogel contact lens composed of quaternized chitosan (HTCC), AgNPs, and graphene oxid (GO) and indicated that the hydrogel is cross-linked through electrostatic interactions between GO and HTCC enhancing mechanical properties and also exhibiting good antimicrobial functions. The spectral transmittance properties of contact lenses Transparency is an essential property of any contact lens-based application. ElShaer et al. [20], synthesized prednisolone-loaded poly (lactic-*co*-glycolic acid) nanoparticles and found that the transmission was decreased by 8% with the increase in drug nanoparticles concentration compared to unloaded contact lenses.

This study aimed to preparation of silicone-hydrogel films incorporated AgNPs and evaluation of their physicomechanical properties, toxicity and *in- vitro* antimicrobial efficacy.

2. Materials and methods

2.1. Materials

Bis-alpha,omega-(methacryloxypropyl)polydimethylsiloxane (MA-PDMS-MA) macromonomer, and 3-Methacryloxypropyl tris (trimethyl soloxy silane) (TRIS) (98%) were purchased from Gelest. *N,N*-dimethyl acrylamide (DMA), ethylene glycol dimethacrylate (EGDMA) and *N*-vinyl pyrrolidone (NVP) were purchased from Merck Co. Photoinitiator Darocur 1173 was purchased from Sigma Co. Silver nitrate was supplied by Sisco Reasearch Laboratories PVT.LTD(Mumbai, India).

2.2. Methods

The SiHCFs were prepared by modifying the synthesis procedure developed by Kim et al [21]. A 3 ml of mixture of TRIS, MA-PDMS-MA and DMA with the ratio 4:1:2 were combined with 0.18 ml of NVP, and 15 µl of EGDMA. Then the mixture was purged with dry nitrogen for 15 min. Silver nitrate dissolved in ethanol (0, 10, 20, 30, 40, 60, 80 ppm) was added to the mixture, transparent brown colour appeared. Finally, 0.3 ml ethanol and 8 mg of photoinitiator Darocur 1173 were added and stirred for 5 min. Then, the mixture was injected into a mold which composed of two 5 mm thick glass plates separated by a silicone composite spacer and subjected to UV lamp of 365 nm for 50 min forming SiHCFs (control, A, B, C, D, E, F) respectively. The hydrogel film was soaked in 70% ethanol overnight to remove the excess of silver nitrate and unreacted monomers then dried in air.

2.3. Characterization

2.3.1. Elucidation of AgNPs formation

2.3.1.1. Transmission electron microscopy. Transmission electron microscopy (TEM) is a microscopy technique. A beam of electrons is transmitted through an ultra-thin specimen, and then interacts with the specimen as it passes through. An image is formed from the interaction of the electrons transmitted through the specimen; and the image is magnified and focused onto an imaging device or detected by a camera. The TEM samples, which used to characterize the nanoparticles by placing a drop of co-polymerizing monomer mixture solution resulting after the addition of 40 ppm $AgNO_3$ solution directly on a carbon coated copper grid (200 meshes). The sample was air dried before TEM examination.

2.3.1.2. UV–Vis spectrophotometry. Preliminary characterization of the formed AgNPs in the hydrogels was carried out using UV–Vis spectroscopy. Usually, AgNPs exhibit unique and tunable optical properties due to their surface plasmon resonance (SPR) that are dependent on shape, size and size distribution of the nanoparticles [22]. UV–vis absorption spectra of co-polymerizing monomers mixture solution formed after addition of (0, 40, 80 ppm) $AgNO_3$ and spectra of SiHCFs (Control, C, D, E, F) were recorded on JASCO V-630 spectrophotometer at the wavelength ranged between 1100–190 nm.

2.3.1.3. Scanning electron microscopy- energy dispersive X-ray spectrometry (SEM-EDX). Back scattered electron images in the SEM display compositional contrast that results from different atomic number elements and their distribution. Energy Dispersive X-ray Spectroscopy (EDX) allows one to identify what those particular elements are and their relative proportions.

The prepared silicone-hydrogel composite (SiHC) samples were analyzed on double-sided tape on aluminum stubs. Micrographs of the surface and the transversal cut were taken using a Quanta FEG250-apparatus coupled with Energy Dispersive X-ray Spectroscopic (Taem EDAX) to elucidate the disruption mode of AgNPs.

2.3.2. Fourier transform infrared spectroscopy

Fourier Transform Infrared spectroscopy (FTIR) is a technique, which is used to obtain an infrared spectrum of absorption, emission, photoconductivity or Raman scattering of a solid, liquid or gas. FTIR is based on the theory that each chemical group has characterized absorption infrared spectrum. FTIR was utilized to study the chemical structure of hydrogel and polymers, interaction of nanoparticles and hydrogel materials. The samples were scanned by FTIR in the range of 600–4000 cm^{-1}.

2.3.3. Thermogravimetric analysis (TGA)

TGA was carried out on a SDTQ 600 thermogravimetric analyzer with heating rate of 10 $^{o}C\ min^{-1}$.

2.3.4. Transparency measurement (Light transmittance)

The optical transparency were conducted by measuring the percent transmittance of visible light (wavelength range from 450 to 750 nm) through swollen films of the prepared SiHC in distilled water using a UV/Vis spectrophotometer (Agilent Technologies, Cary series UV–vis spectrophotometer). The samples were placed between two glass slides (about 0.5 mm thick) and transparency measured at 25 °C.

2.3.5. Mechanical property measurements

A hydrated sample of the prepared SiHCFs (2 × 0.4 cm) was mounted in a Zwick Roell test system. The samples were stretched uniaxial with a load range of 100 N applied on the tensile test and a crosshead speed of 5 mm/min at room temperature. The Young's modulus (E), was measured.

2.4. Antibacterial measurements

2.4.1. Bacterial strains and culture conditions

Gram-negative [*Escherichia coli* (*E. coli,* ATCC- 25922), *Pseudomonas aeruginosa* (*P. aeruginosa*, strain OS4)] and Gram-positive [*Staphylococcus aureus* (*S. aureus*, ATCC-47077)] were used in this study and inoculated from - 20 °C storage into 10 mL of nutrient broth (NB, Difco laboratories, Sparks, MI, USA) and incubated overnight at 37 °C and 30 °C, respectively. The 0.1 mL of bacterial cells were centrifuged at 8000 rpm for 3 min, washed once in phosphate buffer saline (PBS; composed of NaCl 8 g l^{-1}, KCl 0.2 g l^{-1}, Na_2HPO_4 1.44 g l^{-1}, KH_2PO_4 0.24 g l^{-1}; pH 7.2) and re-suspended in 1/1000 NB/PBS. The bacterial cell suspensions were then serially diluted (1/10) and used for adhesion assay.

2.4.2. Bacterial inhibition assay

The prepared SiHCFs were cut into discs and then washed twice with sterile distilled water prior to the assay. The discs were then transferred into 1 ml of bacterial suspension (prepared above) in culture tubes (2 mL) and incubated for 24 h. The diluted culture solution from each test was plated on a nutrient agar (NA) plate for the bacterial counts. Colony forming units (CFU) on the plate were counted, after incubation overnight.

2.4.3. Bacterial adhesion assay

After the study of bacterial inhibition assay on the prepared SiHC discs, they were washed three times in 1 ml PBS (each time shaking for 30 s) to remove loosely bound bacteria, then transferred into a culture tubes containing 2 ml of PBS. The test tubes were then vortexes for 1 min at a maximum speed to allow bacterial cells to detach. The solution from each test was plated on NA plate for the bacterial counts and colony forming units (CFU) on the plate were counted, after incubation overnight.

2.5. Cytotoxicity assay of silicone-hydrogel composites

Cytotoxic activity test (*In- vitro* bioassay) on normal human epithelial amnion cells WISH and fibroplast origin cells BJ1 were conducted and determined by the Bioassay-Cell Culture Laboratory, National Research Centre. Potential cytotoxicity evaluation of biomaterials was examined using the colorimetric method of Mosmann [23]. Cell viability was assessed by the mitochondrial dependent reduction of yellow MTT (3-(4,5-dimethylthiazol-2-yl)-2,5-diphenyl tetrazolium bromide) to purple formazan. This is due in part to dehydrogenase enzymes generating intracellular purple formazan that can be solubilized and quantified by spectrophotometric means. Cells were suspended in RPMI 1640 medium. The media were supplemented with 1% antibiotic-antimycotic mixture (10,000 Uml^{-1} Potassium Penicillin, 10,000 $\mu g\,ml^{-1}$ Streptomycin Sulfate and 25 $\mu g\,ml^{-1}$ Amphotericin B), 1% L-glutamine and 10% fetal bovine serum and kept at 37 °C under 5% CO_2.

Cells were batch cultured for 10 days, then seeded at concentration of 10×10^3 cells/well, determined by cell counting using a haemocytometer, in fresh complete growth medium in 96-well microtiter plastic plates at 37 °C for 24 h under 5% CO_2 using a water jacketed Carbon dioxide incubator (Sheldon, TC2323, Cornelius, OR, USA). Samples were chopped into small pieces, 0.5 g sample per well was added and left to incubate for 24 h under sterile conditions. After 24 h, the samples were removed and the media aspirated. 40 µl of 0.5% MTT solution, sterile filtered through 0.2 µm filter, was added to each well. Wells were made up to 500 µL with cell media and left to incubate for 4 h. The media was aspirated and rinsed twice with sterile PBS. Cells were lyzed and the formazan dissolved with 200 µl of DMSO. 150 µl from each well was pipetted into 96 cell plates. To stop the reaction, 200 µl of 10% Sodium dodecyl sulphate (SDS) in deionized water was added to each well and incubated overnight at 37 °C [24].

The absorbance was then measured using a microplate multi-well reader (Bio-Rad Laboratories Inc., model 3350, Hercules, California, USA) at 595 nm and a reference wavelength of 620 nm A statistical significance was tested between samples and negative control (cells with vehicle) using independent *t*-test by SPSS 11 program. Dimethyl sulphoxide (DMSO) is the vehicle and its final concentration on the cells was less than 0.2%.The percentage of change in viability was calculated according to the following formula:

$$\text{Relative cell viability\%} = \left(\frac{\text{Reading of extract}}{\text{Reading of negative control}} - 1\right) \times 100$$

3. Results and discussion

AgNPs was incorporated into silicone-hydrogel according to the mechanism shown in Fig. 1. Ag ions was reduced by the reducing groups available in the co-polymerizing monomers mixture solution and the methacryloxypropylpolydimethylsiloxane fragments containing carboxylic groups stabilized nanoparticles against agglomerating with each other.

3.1. Characterization

3.1.1. Elucidation of AgNPs formation

3.1.1.1. TEM observation of AgNPs. TEM micrograph of the *in situ* formation of AgNPs by reduction of $AgNO_3$ added at concentration 40 ppm to co-polymerizing monomers mixture was shown Fig. 2. It was clear that AgNPs were in an almost spherical form and appeared to have a core shell like structure.

3.1.1.2. UV–vis absorption spectra of AgNPs. UV–vis absorbance measurements were used to confirm the *in situ* formation of AgNPs in the co-polymerizing monomers mixture solution and in the casted SiHCs and illustrate the size and the concentration of AgNPs as well. The optical spectra of the AgNPs embedded in co-polymerizing monomers mixture solution and SiHCFs were shown in Fig. 3(A,B). It was found that UV–Vis spectra showed characteristic peak at about 400 nm for co-polymerizing monomers mixture solution and casted SiHCFs. Theses peaks have been satisfactorily identified for AgNPs. The

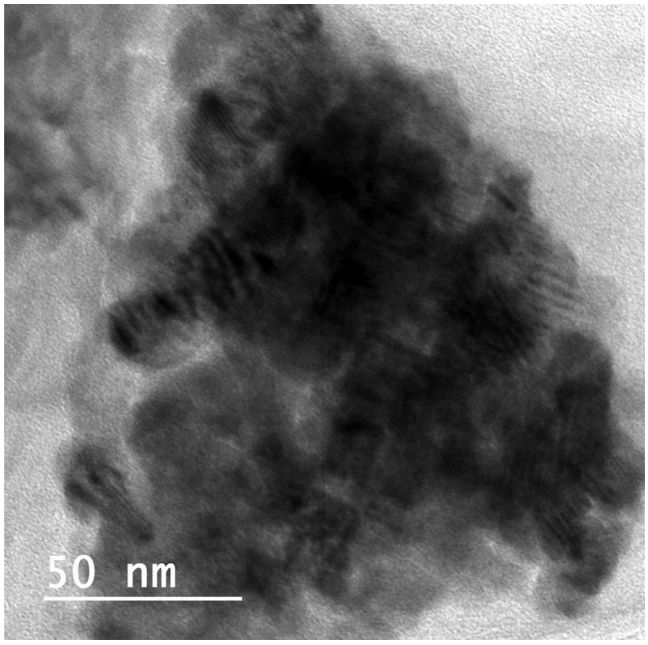

Fig. 2. TEM image of silicone copolymerizing monomers mixture after addition of 40 ppm $AgNO_3$ solution.

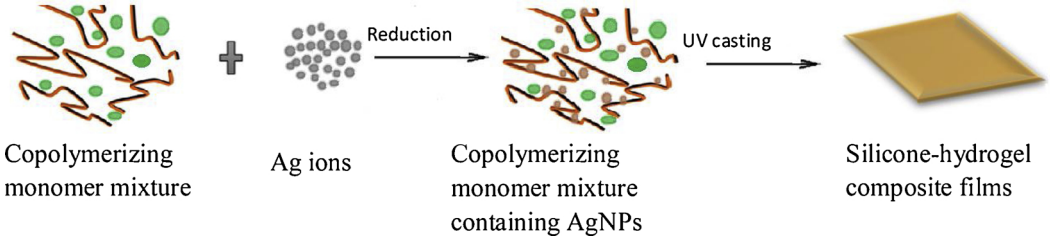

Fig. 1. General scheme for the synthesis of SiHCFs.

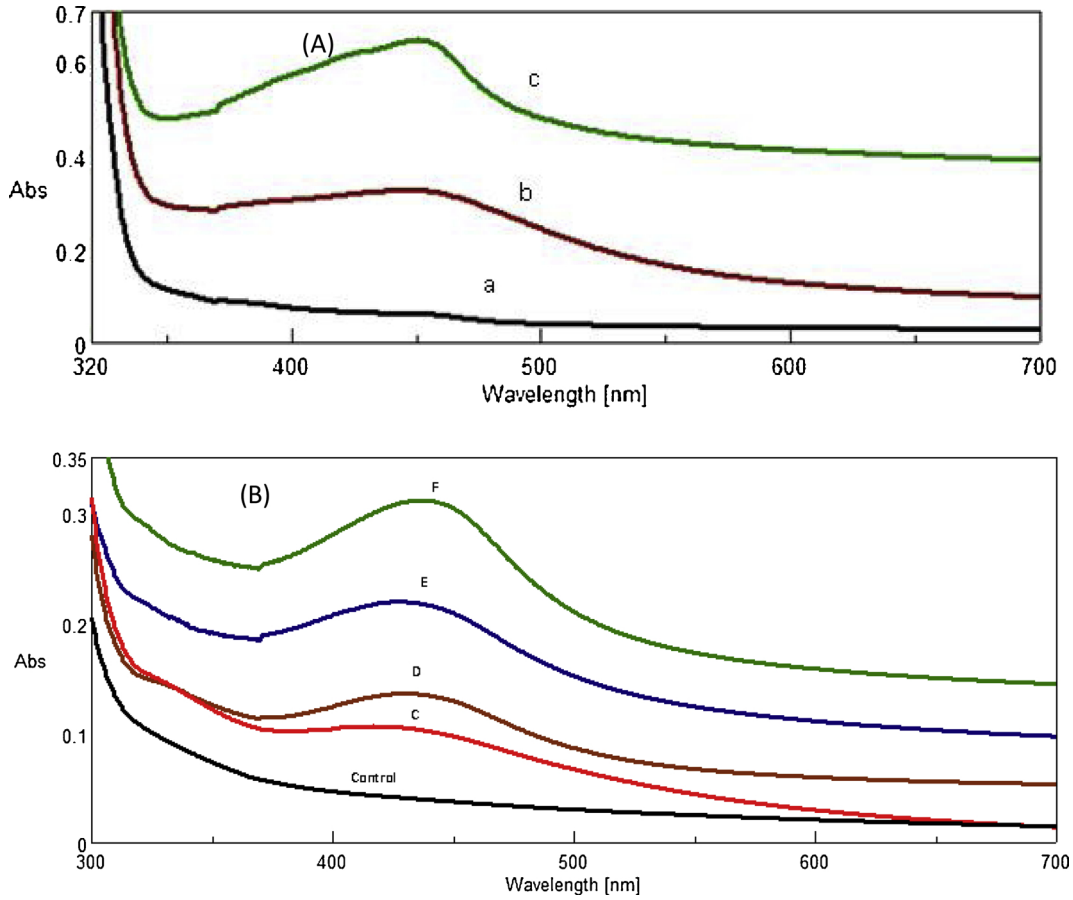

Fig. 3. UV–vis spectra of (A) co-polymerizing monomers mixture solution after addition of a) 0, b) 40, c) 80 ppm $AgNO_3$, (B) the prepared SiHCFs (control, C, D, E, F).

bandwidth, the intensity and the position of peaks also increased when the AgNPs fraction increased.

3.1.1.3. Scanning electron microscope (SEM) and energy-dispersive X-ray spectroscopy (EDX) of SiHCFs. The presence of silver element in SiHCFs can be evidenced by the SEM and EDX mapping. Fig. 4 showed the SEM of SiHCF (D), while Fig. 5 demonstrated EDX mapping of the elements from SiHCFs (D, F). The dots of (a,b), (c), (d),(e) and (f) shown in Fig. 5 were the elements of AgNPs, C, N, O and Si from the investigated SiHCFs (D) and (F) respectively.

It was clear that SEM and EDX mapping confirmed the successful synthesis of AgNPs into the SiHCFs and AgNPs were well homogenously dispersed into the polymer matrices of SiHCFs and became to aggregate slightly with increasing their concentration.

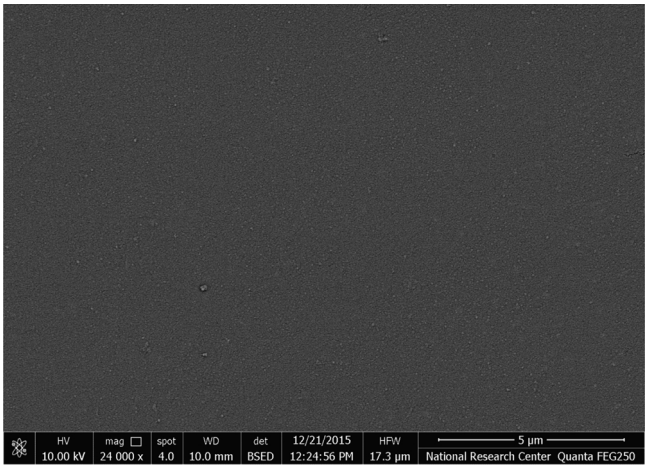

Fig. 4. Surface section of SEM images of the prepared SiHCF (D) at 24,000 x magnifications.

3.1.2. FTIR analysis

Fig. 6(a) demonstrated the FTIR spectra of SiHCFs (control,C,D,E,F). The all bands at 1740 cm^{-1}, 1665 cm^{-1}, 1277 cm^{-1} and 1146 cm^{-1} stand for the vibration of C═O group. The band around 2957 cm^{-1} belongs to the stretching vibration of C—H from the prepared silicone-hydrogel composites. C—N has the absorption band at 1453 cm^{-1}. Also, it was clear that there was no difference between silicone-hydrogel (control) and silicone-hydrogels incorporated AgNPs.

3.1.3. The thermal properties of composites

The thermogravimetric analysis (TGA) of the SiHCFs (control, F) were shown in Fig. 6(b). It was found that, at higher loadings of AgNPs, the SiHC (F) exhibited the same trend towards thermal stability. This revealed that the highest concentration of AgNPs did not cause any change on the structure of the silicone-hydrogel matrix.

3.1.4. Ophthalmic characterization

The optical transmittance of the prepared SiHCFs were represented in Fig. 6(c). It was clear that all SiHCFs at wavelength range 750–550 nm exhibited transmittance greater than 90%. The transmittance at 500 nm was greater than 84% for all SiHCFs. Although the transmission of SiHCFs (A,B,C,D) at 450 nm observed above 85%, the transmissions of SiHCFs (E, F) declined sharply to 72.23 and 64.6 nm respectively owing to the increase of AgNPs loading in lattice structure.

3.1.5. Mechanical properties

Fig. 6(d) illustrated the Young's modulus of the prepared SiHCFs

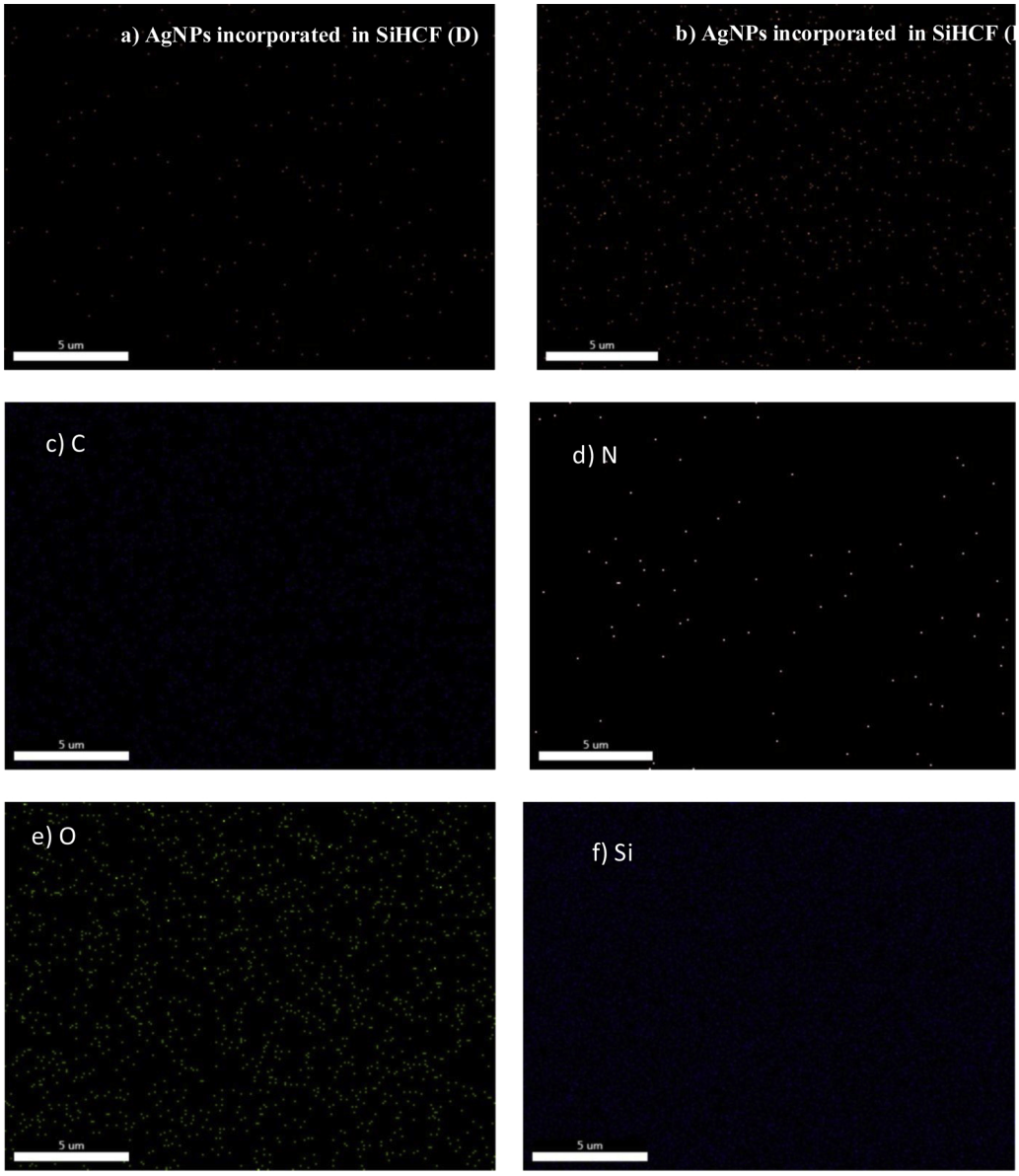

Fig. 5. EDX mapping micrograph of (a,b) AgNPs, (c) C, (d) N and (e) O and (f) Si of the prepared SiHCFs (D and E).

(control, C, D, E and F). It was found that the AgNPs loading increased Young's modulus from 1.06 to 1.38 MPa.

3.2. Antibacterial study on the prepared SiHCs

3.2.1. Inhibition of bacterial growth assay

The reduction of bacteria growth for *E.coli, P.aeruginosa* and *S.aureus* in solution containing the SiHC discs were illustrated in Fig. 7(a). It was noticeable that SiHC disc, (control), revealed no antibacterial activities against *E.coli, P.aeruginosa* or *S.aureus* strains after 24 h. However, the antimicrobial activity of SiHCs were significantly enhanced by incorporation of AgNPs. The relative number of bacterial growth in PBS surrounding SiHC discs (control,A,B,C,D,E,F) was to be 95, 78, 4, 2, 0, 0, 0% for *E.coli*, 95, 82, 4, 0.6, 0, 0, 0% for *P. aeruginosa*, and 93, 79, 4, 0.5, 0, 0, 0% for *S. aureus* respectively. This indicated that the AgNPs were released into the solution surrounding the SiHC discs during incubation to be active against the bacteria causing sharp declines of bacteria growth. Additionally, SiHC discs (B,C,D,E,F) showed almost total kill of bacterial cells of the all strains in the PBS.

Comparing the inhibition behaviors of bacteria growth for the three strains (*E.coli, P.aeruginosa* and *S.aureus*), it was found that there were no significant differences in the inhibition extents of all strain.

3.2.2. Bacterial adhesion assay

The number of adhered cells of *E.coli, P.aeruginosa* and *S.aureus* on the SiHC discs were presented in Fig. 7(b). According to our results, there was a dose dependent response to the amount of AgNPs incorporated into the SiHC discs. SiHC discs (A,B,C) loaded with AgNPs to an extent sufficiently to kill about from 20% to 55% of microbes only, whereas SiHC discs (D,E,F) holding higher concentrations of AgNPs had ability to give remarkable antibacterial properties against *E.coli, P.aeruginosa* and *S.aureus*. Additionally, our data revealed that AgNPs could highly inhibit the formation of such bacterial biofilms on the SiHC surface. Moreover, it was obvious that *P.aeruginosa* strain showed the highest reduction growth compared to *E.coli* and *S.aureus*.

The *in- vitro* antibacterial assays demonstrated limited and/or prevented bacterial contamination of the prepared SiHCFs containing AgNPs.

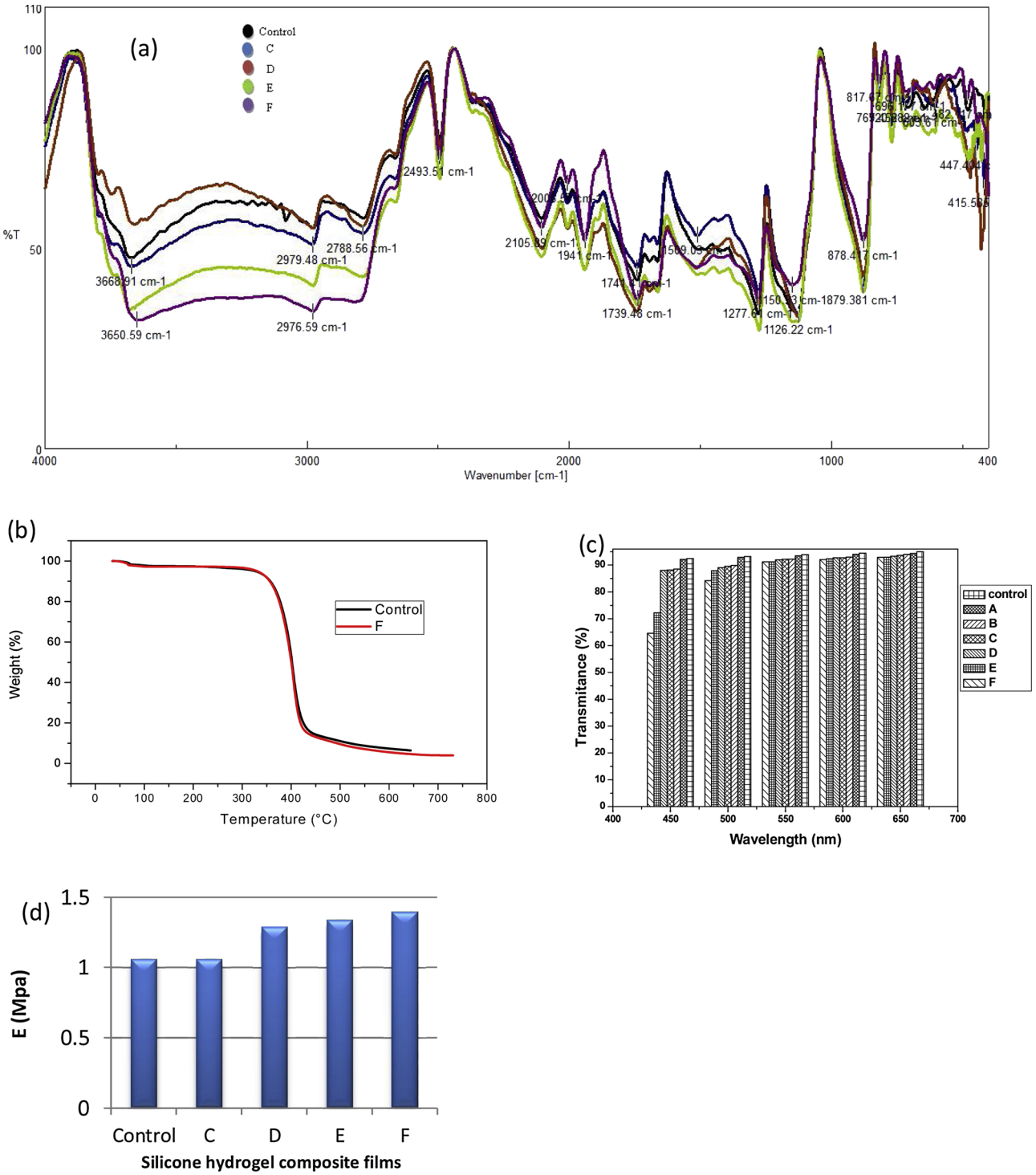

Fig. 6. (a) FTIR of the prepared SiHCFs (control, C, D, E, F), (b)Thermogravimetric analysis of the prepared SiHCFs (control, F), (c) Transparency of the prepared SiHCFs (control,A,B, C, D, E and F), (d) The Young's modulus of the prepared SiHCFs (control, C, D, E and F).

3.3. Cytotoxicity assay

The biocompatibility of the SiHCs is one of the most important criteria to be applied as contact lens materials and/or other body implants. Fig. 8(a,b) indicated that the viability of cells WISH and BJ1 treated with SiHC samples (control,D,E,F) were 96.3%,86.7%, 84%, 81% and 92%, 91%, 89%, 83.3% respectively. SiHC sample (control) showed the highest cell viability which confirmed that silicone-hydrogel is a biocompatible material. A significant finding that all human epithelial amnion and fibroblast cells seeded were alive after 24 h incubation. Moreover, the relative cell viability was higher than 80%. These results suggested that these SiHCs were likely not substantially cytotoxic to tested cells and the release of AgNPs did not succeed to the extent generating toxicity.

4. Discussion

It was clear from TEM image (Fig. 2), AgNPs were encapsulated in co-polymerizing monomers mixture while polydimethylsiloxane macromer stabilized or encapsulated them [25]. It has been stated that the

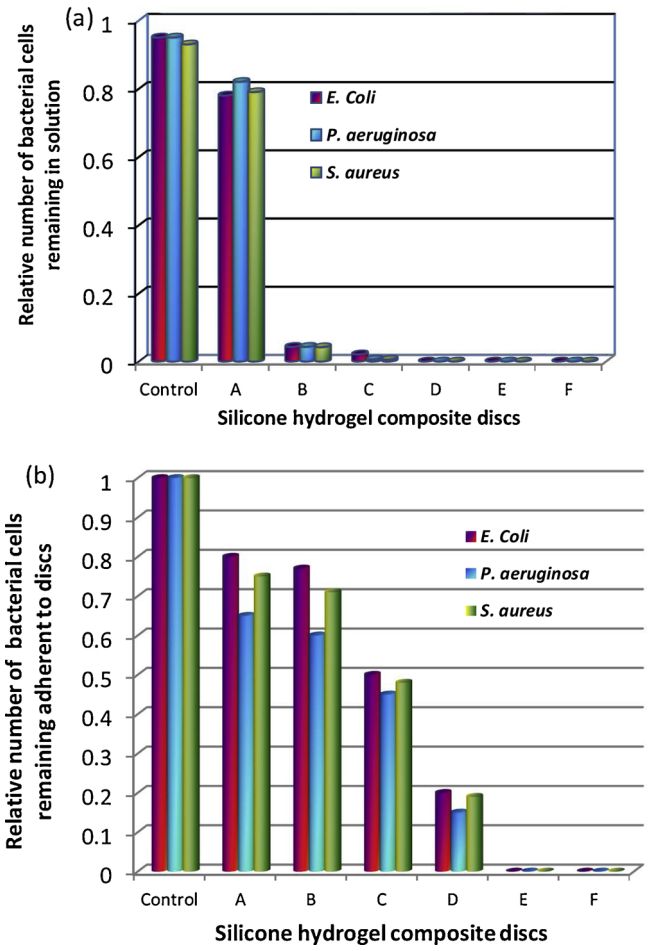

Fig. 7. (a)Reduction in growth of microbial cells in the solution surrounding the prepared SiHC discs (control, A, B, C, D, E and F), (b) Reduction in adhesion of microbial cells on the prepared SiHC discs (control, A, B, C, D, E and F).

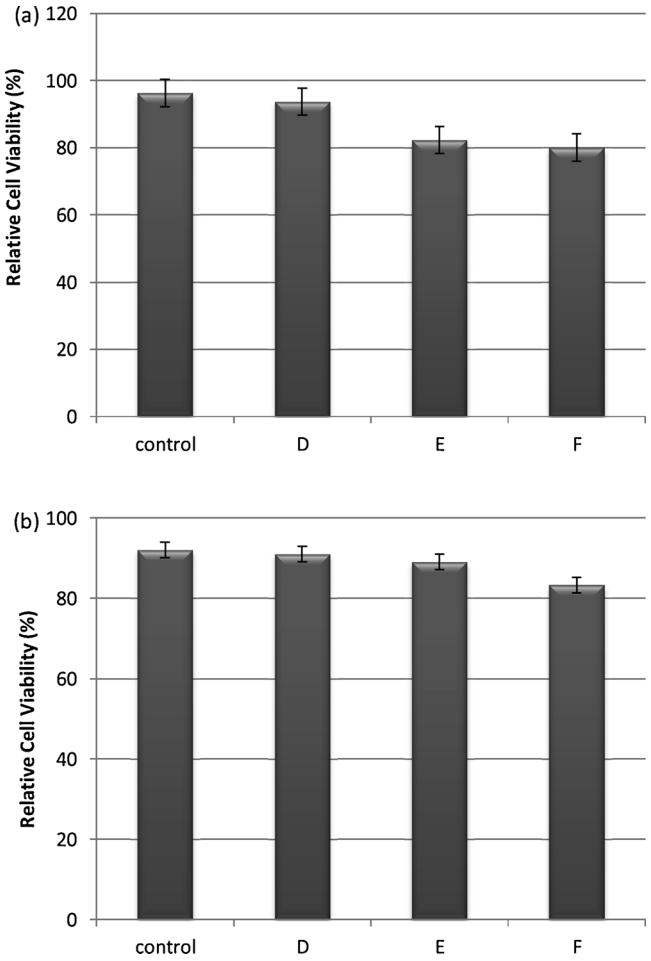

Fig. 8. (a) Cell viability of human epithelial amnion cells WISH, (b) Cell viability of fibroplast origin cells BJ1 on the prepared SiHCs (control, A, B, C, D, E and F).

natural and synthetic polymers can act as stabilizers for metal nanoparticles [26,27].

It was found that, from the UV–Vis spectra (Fig. 3), the characteristic surface plasmon resonance (SPR) of the AgNPs assigned peak at about 400 nm for co-polymerizing monomers mixture solution and also for SiHCFs that has been properly identified for AgNPs with various sizes ranging from 2 to 100 nm [28]. Moreover, the bandwidth, the intensity and the position of peaks also increased when the AgNPs fraction increased. The small particles were very unstable in the solution and they tended to aggregate onto the surface of other silver particles, which led to increase the size of some silver particles [29]. Therefore, the size of AgNPs became non-uniform after casting process as shown from SEM and EDX mapping images (Figs. 4,5). Additionally, the volume fraction, the shape and the size of AgNPs in the co-polymerizing monomers mixture and SiHCFs, as well as the interparticle separation and the dielectric properties of the surrounding medium influenced the bandwidth, the intensity and the position of the surface-plasmon resonance wavelength of the nanocomposite material [30,31]. The increase in the fraction of silver led to the decrease in the interparticle spacing resulting in the red shift of the SPR's peak position [31–33].

The SiHCFs at wavelength range 750 - 550 nm shown in Fig. 6c exhibited transmittance greater than 90% then followed by reduction to be about 84% at 450 nm but, SiHCFs samples (E and F) manifested sharp decline in transmission at 450 nm to 72.23 and 64.6 nm respectively. It has been reported that the visible-light transmittance of over 90% at 600 nm satisfies the visual requirements for all contact lenses [34]. The yellow and green light that have wavelength around 555 nm are distinguishable for human eye [35]. Therefore, SiHCFs were suitable for ophthalmic biomaterial. The observed reduction in transmission was due to aggregation of the AgNPs, which scattered light, and caused the loss of transparency [36] and appearance of the strong absorption peak of AgNPs in the range 400–500 nm [37] and its intensity increased as its loading increased as shown from UV–vis absorption section. Gulsen and Chauhan [36], measured the transparency of the pure p-HEMA and microemulsion loaded p-HEMA hydrogels at 600 nm and found transmittance for the pure p-HEMA hydrogel was about 87% and the hydrogels formed by polymerization of microemulsion added to p-HEMA were opaque and recorded transmittance of about 79%, 69% and even to 19% and 4.4%. ElShaer et al. [20], indicated that the incorporation of 0.2 g and 0.4 g of Prednisolone NPs into poly (lactic-*co*-glycolic acid) lowered the transmission at 600 nm to 86.23% and 83.1%, respectively. Therefore, this study indicated the incorporation of AgNPs into SiHCFs would not affect the transparency at 600 nm.

Young's modulus (E) is considered a critical and an important property of contact lenses for vision and its safty [38]. The modulus values were in the range of commercial silicone-hydrogels that around 0.5–1.5 MPa [39]. As a consequence, the stiffer SiHCs did not drape over the cornea and had excellent handling characteristics [21,40]. The addition of AgNPs resulted in slight increase in the Young's modulus but their values ranging from 1.06 to 1.38 MPa as indicated in Fig. 6d still less than the value (1.44 MPa) of marketed silicone-hydrogels (CIBA Vision's Focus Night & Daymaterial, lotrafilcon A) [40].

It has been reported that *Staphylococcusepidermidis, Staphylococcus*

aureus, Enterobacter and *Pseudomonas* species were the most common microorganisms detected on soft contact lenses [41]. *Acanthamoeba* keratitis were also more observed in contact lenses wearers, probably as a result of the contaminated tap water used for the lens care [42,43]. Kamel and Norazah [44], found *Acanthamoeba* keratitis as the first case of in a female's contact lens. *Acanthamoeba* keratitis might resulted from bacteria found in eyelids, conjunctiva and tear film [43]. Emina and Idu [42], found that *E. coli* was more in the extended silicone-hydrogel contact lens. This work might provide appropriate method in order to reduce the degree of microbial contamination for extended silicone contact lens wearers.

It was obvious that the amount of AgNPs into silicone-hydrogel was important to give proper antimicrobial efficacy. Rad et al. [16], demonstrated that remarkable inhibitory effects of AgNPs impregnated poly (HEMA) soft contact lens against *P. aeruginosa* and *S. aureus* after soaking in 10 and 20 ppm AgNPs suspension, but 2 ppm AgNPs loading was not enough for bacterial inhibitory effects. In previous study by Bazzaz et al. [6], showed satisfactory inhibitory effects of AgNPs against *P. aeruginosa* and *S. aureus* when incorporated in soft contact lens proxies during polymerization process. Willcox et al. [45], reported the ability of AgNPs to overcome the bacterial growth of *S. aureus*, *P. aeruginosa* and *Acanthamoeba castellanii* and reduced the adhesion to etafilcon A contact lens surface after soaking in 10 and 20 ppm AgNPs suspension. Other study demonstrated that fimbrolides covalently coated Lotrafilcon A contact lenses reduced the adhesion of *P. aeruginosa* and *S. aureus* with about 67% and 92% respectively. Willcox et al. [46], found that the cationic peptide Melimine covalently incorporated into etafilcon A lenses decreased the adhesion of *P. aeruginosa* by 92% and of *S. aureus* by 76%. According to our findings, the inhibitory adhesion effect of AgNPs loaded silicone-hydrogel was significantly increased with increasing the amount AgNPs to be between 20%–100%, 35%–100 % and 25%–100% for *E.coli*, *P. aeruginosa* and *S. aureus* respectively (Fig. 7b).

The current study demonstrated that the prepared silicone-hydrogel/ AgNPs composites showed less antibacterial actions than that produced in the previous work [15]. This can be attributed to the sliver nanoparticles produced by incorporation in silicone-hydrogel matrices maybe more tightly bonded and diffused into the matrices than that impregnated on the surface of silicone-hydrogels resulting in less amount of silver released into the culture media and consequently may exhibit less toxic effects. This is in agreement with the observations from the UV–vis spectra, SEM and EDX mapping images.

A key finding of this study was the preparation of silicone hydogel containing AgNPs that did not show toxicity yet that did exhibit antimicrobial activity without affecting its native features managing them to be applicable as contact lenses. The characteristics of silicone-hydrogel lenses such as transparency, flexibility and swelling maybe affected by addition of high concentration of AgNPs. As reported in other studies, the exposure to higher amounts of silver may result in undesirable ocular significances such as argyrosis [47]. Ocular argyrosis depends on the amount and duration of exposure to the silver [48–50]. Willcox et al. [45], soaked etafilcon A lenses in various AgNPs concentrations, found the excellent antimicrobial effects at 20 ppm and stated that this amount could not cause argyrosis in continuous lens wearers for many years.

Our data revealed that AgNPs did not impose toxicity and could highly overcome bacterial biofilm formation that is consequently considered general problems of eye infections and inflammations for soft contact lens wearers.

5. Conclusions

The SiHCFs were synthesized by the reduction of silver nitrate added to copolymerizing monomers mixture followed by film casting.

UV-Vis absorption and TEM ascertained the presence of AgNPs in copolymerizing monomers mixture. FTIR and TGA of SiHCFs showed that the presence of AgNPs did not influence the network structure. The shape and distribution of AgNPs incorprted into SiHCFs were realized by UV–vis absorption, SEM and EDX mapping. The incorporation of AgNPs into the SiHCFs improved the tensile modulus and decreased the transmittance but still greater than 90% at 600 nm. Moreover, the antimicrobial assay demonstrated that the prepared SiHCFs had potent antimicrobial inhibitory without revealing toxicity.

Declaration of interests

The authors report no conflicts of interest. The authors alone are responsible for the content and writing of the paper.

Acknowledgement

We are grateful to National Research Centre for financial support.

References

[1] B.V. Slaughter, S.S. Khurshid, O.Z. Fisher, A. Khademhosseini, N.A. Peppas, Hydrogels in regenerative medicine, Adv Mater 21 (32–33) (2009) 3307–3329.
[2] M. Green, A. Apel, F. Stapleton, Risk factors and causative organisms in microbial keratitis, Cornea 27 (1) (2008) 22–27.
[3] Y.M. Por, J.S. Mehta, J.L. Chua, T.-H. Koh, W.B. Khor, A.C. Fong, et al., Acanthamoeba keratitis associated with contact lens wear in Singapore, Am J Ophthalmol 148 (1) (2009) 7–12.
[4] J. Sengupta, S. Saha, A. Khetan, S.K. Sarkar, S.M. Mandal, Effects of lactoferricin B against keratitis-associated fungal biofilms, J Infect Chemother 18 (5) (2012) 698–703.
[5] M.D. Willcox, Review of resistance of ocular isolates of Pseudomonas aeruginosa and staphylococci from keratitis to ciprofloxacin, gentamicin and cephalosporins, Clin Exp Ophthalmol 94 (2) (2011) 161–168.
[6] B.S.F. Bazzaz, B. Khameneh, M.-m. Jalili-Behabadi, B. Malaekeh-Nikouei, S.A. Mohajeri, Preparation, characterization and antimicrobial study of a hydrogel (soft contact lens) material impregnated with silver nanoparticles, Contact Lens Anterior Eye 37 (3) (2014) 149–152.
[7] R.E. Weisbarth, M.M. Gabriel, M. George, J. Rappon, M. Miller, R. Chalmers, et al., Creating antimicrobial surfaces and materials for contact lenses and lens cases, Eye Contact Lens 33 (6, Part 2 of 2) (2007) 426–429.
[8] H. Zhu, A. Kumar, J. Ozkan, R. Bandara, A. Ding, I. Perera, et al., Fimbrolide-coated antimicrobial lenses: their in vitro and in vivo effects, Optom Vis Sci 85 (5) (2008) 292–300.
[9] W. Huang, R. Zhang, G. Zou, J. Tang, J. Sun, An iodide/anion exchange route to benzimidazolylidene silver complexes from benzimidazolium iodide: crystal structures of N, N′-dibutylbenzimidazolylidene silver chloride, bromide, cyanide and nitrate, J Organomet Chem 692 (17) (2007) 3804–3809.
[10] A.R. Knapp, M.J. Panzner, D.A. Medvetz, B.D. Wright, C.A. Tessier, W.J. Youngs, Synthesis and antimicrobial studies of silver N-heterocyclic carbene complexes bearing a methyl benzoate substituent, Inorganica Chim Acta 364 (1) (2010) 125–131.
[11] G. Roymahapatra, S.M. Mandal, W.F. Porto, T. Samanta, S. Giri, J. Dinda, et al., Pyrazine functionalized Ag (I) and Au (I)-NHC complexes are potential antibacterial agents, Curr Med Chem 19 (24) (2012) 4184–4193.
[12] V. Kumar, C. Jolivalt, J. Pulpytel, R. Jafari, F. Arefi-Khonsari, Development of silver nanoparticle loaded antibacterial polymer mesh using plasma polymerization process, J Biomed Mater Res A 101 (4) (2013) 1121–1132.
[13] L. Ploux, M. Mateescu, K. Anselme, K. Vasilev, Antibacterial properties of silver-loaded plasma polymer coatings, J Nanomater 2012 (2012), https://doi.org/10.1155/2012/674145.
[14] M. Ahamed, M.S. AlSalhi, M. Siddiqui, Silver nanoparticle applications and human health, Clin Chim Acta 411 (23–24) (2010) 1841–1848.
[15] F. Helaly, S. El-Sawy, A. Hashem, A. Khattab, R. Mourad, Synthesis and characterization of nanosilver-silicone-hydrogel composites for inhibition of bacteria growth, Cont Lens Anterior Eye 40 (1) (2017) 59–66.
[16] M. Shayani Rad, B. Khameneh, Z. Sabeti, S.A. Mohajeri, B.S. Fazly Bazzaz, Antibacterial activity of silver nanoparticle-loaded soft contact lens materials: the effect of monomer composition, Curr Eye Res 41 (10) (2016) 1286–1293.
[17] K. Haraguchi, R. Farnworth, A. Ohbayashi, T. Takehisa, Compositional effects on mechanical properties of nanocomposite hydrogels composed of poly (N, N-dimethylacrylamide) and clay, Macromolecules 36 (15) (2003) 5732–5741.
[18] X. Zhao, Q. Zhang, D. Chen, P. Lu, Enhanced mechanical properties of graphene-based poly (vinyl alcohol) composites, Macromolecules 43 (5) (2010) 2357–2363.
[19] J.-F. Huang, J. Zhong, G.-P. Chen, Z.-T. Lin, Y. Deng, Y.-L. Liu, et al., A hydrogel-based hybrid theranostic contact lens for fungal keratitis, ACS Nano 10 (7) (2016) 6464–6473.
[20] A. ElShaer, S. Mustafa, M. Kasar, S. Thapa, B. Ghatora, R.G. Alany, Nanoparticle-laden contact lens for controlled ocular delivery of prednisolone: formulation optimization using statistical experimental design, Pharmaceutics 8 (2) (2016), https://doi.org/10.3390/pharmaceutics8020014.
[21] J. Kim, A. Conway, A. Chauhan, Extended delivery of ophthalmic drugs by silicone-

hydrogel contact lenses, Biomaterials 29 (14) (2008) 2259–2269.
[22] P. Mulvaney, Surface plasmon spectroscopy of nanosized metal particles, Langmuir 12 (3) (1996) 788–800.
[23] T. Mosmann, Rapid colorimetric assay for cellular growth and survival: application to proliferation and cytotoxicity assays, J Immunol Methods 65 (1-2) (1983) 55–63.
[24] M. Thabrew, R.D. Hughes, I.G. MC Farlane, Screening of hepatoprotective plant components using a HepG2 cell cytotoxicity assay, J Pharm Pharmacol 49 (11) (1997) 1132–1135.
[25] E. Abdel-Halim, S.S. Al-Deyab, Utilization of hydroxypropyl cellulose for green and efficient synthesis of silver nanoparticles, Carbohydr Polym 86 (4) (2011) 1615–1622.
[26] A. Henglein, B. Ershov, M. Malow, Absorption spectrum and some chemical reactions of colloidal platinum in aqueous solution, J Phys Chem 99 (38) (1995) 14129–14136.
[27] Y. Shiraishi, N. Toshima, Oxidation of ethylene catalyzed by colloidal dispersions of poly (sodium acrylate)-protected silver nanoclusters, Colloids Surf A Physicochem Eng Asp 169 (1-3) (2000) 59–66.
[28] K.G. Stamplecoskie, J.C. Scaiano, Light emitting diode irradiation can control the morphology and optical properties of silver nanoparticles, J Am Chem Soc 132 (6) (2010) 1825–1827.
[29] H. Kurita, A. Takami, S. Koda, Size reduction of gold particles in aqueous solution by pulsed laser irradiation, Appl Phys Lett 72 (7) (1998) 789–791.
[30] L.L. Beecroft, C.K. Ober, Nanocomposite materials for optical applications, Chem Mat 9 (6) (1997) 1302–1317.
[31] K.L. Kelly, E. Coronado, L.L. Zhao, G.C. Schatz, The optical properties of metal nanoparticles: the influence of size, shape, and dielectric environment, J Phys Chem B 107 (2003) 668–677.
[32] M. Logar, B. Jancar, D. Suvorov, In situ synthesis of Ag nanoparticles in polyelectrolyte multilayers, Nanotechnology 18 (32) (2007), https://doi.org/10.1088/0957-4484/18/32/325601.
[33] S. Hazra, A. Gibaud, C. Sella, Tunable absorption of Au–Al 2 O 3 nanocermet thin films and its morphology, Appl Phys Lett 85 (3) (2004) 395–397.
[34] C.-F. Lai, J.-S. Li, Y.-T. Fang, C.-J. Chien, C.-H. Lee, UV and blue-light anti-reflective structurally colored contact lenses based on a copolymer hydrogel with amorphous array nanostructures, RSC Adv 8 (8) (2018) 4006–4013.
[35] J. Xu, W. Zhu, L. Jiang, J. Xu, Y. Zhang, Y. Cui, Carbazole-grafted silicone-hydrogel with a high refractive index for intraocular lens, RSC Adv 5 (89) (2015) 72736–72744.
[36] D. Gulsen, A. Chauhan, Dispersion of microemulsion drops in HEMA hydrogel: a potential ophthalmic drug delivery vehicle, Int J Pharm 292 (1-2) (2005) 95–117.
[37] S. Mandal, S.K. Arumugam, R. Pasricha, M. Sastry, Silver nanoparticles of variable morphology synthesized in aqueous foams as novel templates, Bull Mater Sci 28 (5) (2005) 503–510.
[38] C.R. Horst, B. Brodland, L.W. Jones, G.W. Brodland, Measuring the modulus of silicone-hydrogel contact lenses, Optom Vis Sci 89 (10) (2012) 1468–1476.
[39] P.C. Nicolson, R.C. Baron, P. Chabrecek, A. Domschke, H.J. Griesser, A. Ho et al., Extended wear ophthalmic lens, Google Patents, 1998.
[40] C.-H. Lin, W.-C. Lin, M.-C. Yang, Fabrication and characterization of ophthalmically compatible hydrogels composed of poly (dimethyl siloxane-urethane)/Pluronic F127, Colloids Surf B Biointerfaces 71 (1) (2009) 36–44.
[41] P.R. Sankaridurg, S. Sharma, M. Willcox, T.J. Naduvilath, D.F. Sweeney, B.A. Holden, et al., Bacterial colonization of disposable soft contact lenses is greater during corneal infiltrative events than during asymptomatic extended lens wear, J Clin Microbiol 38 (12) (2000) 4420–4424.
[42] M.O. Emina, F.K. Idu, Bacteria and parasites in contact lenses of asymptomatic wearers in Nigeria, J Optom 4 (2) (2011) 69–74.
[43] D. Larkin, D. Easty, External eye flora as a nutrient source forAcanthamoeba, Ger J Ophthalmol 228 (5) (1990) 458–460.
[44] A.M. Kamel, A. Norazah, First case of Acanthamoeba keratitis in Malaysia, Trans R Soc Trop Med Hyg 89 (6) (1995) 652.
[45] M.D. Willcox, E.B. Hume, A.K. Vijay, R. Petcavich, Ability of silver-impregnated contact lenses to control microbial growth and colonisation, J Optom 3 (3) (2010) 143–148.
[46] M. Willcox, E. Hume, Y. Aliwarga, N. Kumar, N. Cole, A novel cationic-peptide coating for the prevention of microbial colonization on contact lenses, J Appl Microbiol 105 (6) (2008) 1817–1825.
[47] N.R. Panyala, E.M. Peña-Méndez, J. Havel, Silver or silver nanoparticles: a hazardous threat to the environment and human health? J Appl Biomed 6 (3) (2008) 117–129.
[48] A.P. Moss, M. Sugar, M. Hargett, Effects of occupational argyrosis, Arch Ophthalmol 97 (1979) 906–908.
[49] M.W. Scroggs, J.S. Lewis, A.D. Proia, Corneal argyrosis associated with silver soldering, Cornea 11 (3) (1992) 264–269.
[50] S.C. Hau, S.J. Tuft, Presumed corneal argyrosis from occlusive soft contact lenses: a case report, Cornea 28 (6) (2009) 703–705.